We are IntechOpen, the world's leading publisher of Open Access books Built by scientists, for scientists

6,900
Open access books available

185,000
International authors and editors

200M
Downloads

Our authors are among the

154
Countries delivered to

TOP 1%
most cited scientists

12.2%
Contributors from top 500 universities

WEB OF SCIENCE™

Selection of our books indexed in the Book Citation Index in Web of Science™ Core Collection (BKCI)

Interested in publishing with us?
Contact book.department@intechopen.com

Numbers displayed above are based on latest data collected.
For more information visit www.intechopen.com

25

Design of Non-Uniformly Excited Linear Slot Arrays Fed by Coplanar Waveguide

JP Jacobs, J Joubert and JW Odendaal
University of Pretoria
South Africa

1. Introduction

Slot dipole antennas fed by coplanar waveguide (CPW) have a number of appealing characteristics that include relatively low feed line dispersion and losses at millimeter-wave frequencies, ease of integration with circuit components due to the uniplanar configuration, and considerably wider impedance bandwidth than microstrip patch antennas on comparable substrates, *e.g.*, (Miao et al., 2000). In the sub-millimeter and millimeter-wave ranges, CPW-fed slots have been used to feed dielectric lens antennas (Focardi et al., 2002); arrays of CPW-fed slots are also expected to be used for space applications (Neto et al., 2003).

While a variety of CPW-fed slot arrays have been reported (see section 3), rigorous design procedures for CPW-fed slot arrays that incorporate the effects of element interactions in the form of mutual coupling have only rarely been presented (Huang et al., 1999; Jacobs & Joubert, 2009b). An iterative design typically involves the *a priori* generation of self-admittance data for representative slot dimensions, and requires the calculation of mutual coupling between all possible slot pairs in the array; this is especially pertinent if a non-uniform aperture distribution aimed at achieving reduced sidelobe levels is to be realized.

In this chapter an overview of the current state-of-the-art in the design of non-uniform linear CPW-fed antennas, as well as its subsidiary calculations, is presented. In section 2, the field distribution in an isolated CPW-fed is shown; this is important information for the calculation of mutual coupling. Section 3 focuses on the calculation of mutual coupling using a reciprocity-based paradigm. This is done in the context of two important practical cases. The first involves mutual coupling between slots on electrically thin substrates, where a simplified yet accurate method can be used that obviates use of the substrate Green's function. Arrays of slots on such substrates exhibit bi-directional radiation. The second involves an extended reciprocity approach for calculating the mutual admittance between slots on a conductor-backed two-layer substrate, a configuration that would be useful when unidirectional radiation is required. Section 4 gives details of two types of CPW-fed linear array design. First, the iterative design using an approximate procedure of a uniform array on a conductor-backed two-layer substrate is summarized; measured results are presented. The procedure doesn't require the explicit calculation of the mutual admittance between

pairs of slots, but does take such interactions into account through full-wave calculations of the input impedance of the array as a whole. Second, the implementation of a rigorous iterative design procedure for a non-uniform array with reduced sidelobe levels on an electrically thin substrate is described; measured sidelobe levels of about 16 dB below the main beam were achieved. Due to the electrically thin substrate, the design procedure could draw on the simplified method for calculating mutual admittance outlined in section 3. Section 5 briefly summarizes some of the main findings.

2. Field properties of isolated CPW-fed slots

CPW-fed slots are normally operated in the vicinity of their second resonances because of the favourable impedance bandwidth properties here (compared to the first-resonant region). A CPW-fed slot on a single dielectric layer is shown in Fig. 1. In order to more accurately account for its use in a linear array environment (see Fig. 4), the slot is terminated in a perfect short-circuit realized by a section of transmission line of length l_s.

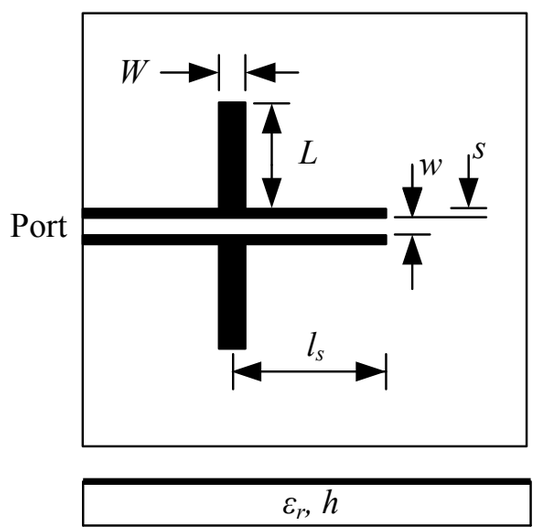

Fig. 1. Top and side views of CPW-fed slot on single-layer substrate. $L \equiv$ half-length and $W \equiv$ width of radiating slot; $s \equiv$ slot width and $w \equiv$ center strip width of CPW feed line; $h \equiv$ dielectric layer height; $\varepsilon_r \equiv$ relative dielectric constant; $l_s \equiv$ length of CPW stub implementing short-circuit.

When evaluating the mutual admittance between pairs of slots, the aperture electric field distribution is required (see section 3). IE3D (Zeland Software, 2001), a full-wave electromagnetic simulator that employs magnetic current modeling and assumes laterally infinite ground planes and dielectrics, can be used to obtain this information. Figs. 2 and 3 (Jacobs & Joubert, 2009a) show magnitudes and phases at 6 GHz of the tangential electric fields along longitudinal slot centers of three isolated slots on an electrically thin substrate with h = 1.575 mm and ε_r = 2.33 (at 6 GHz, h = $0.048\lambda_d$ = $0.0315\lambda_0$, with λ_d and λ_0 the wavelengths in the dielectric and free space respectively). The slots' widths W was 1 mm, their half-lengths L were in the vicinity of the second-resonant half-length L_{res} = 21. 75 mm,

and the length of the short-circuit stub l_s was $0.48\lambda_{CPW}$ = 19.4 mm. The slots were fed by a 87 Ω CPW feed line that had dimensions w = 3 mm and s = 1 mm. (The same radiating slot and feed line dimensions were used in obtaining the mutual admittance results of Figs. 6–8.) The aperture field vector component shown is the one directed across the width of the slot; the orthogonal component was negligible by comparison.

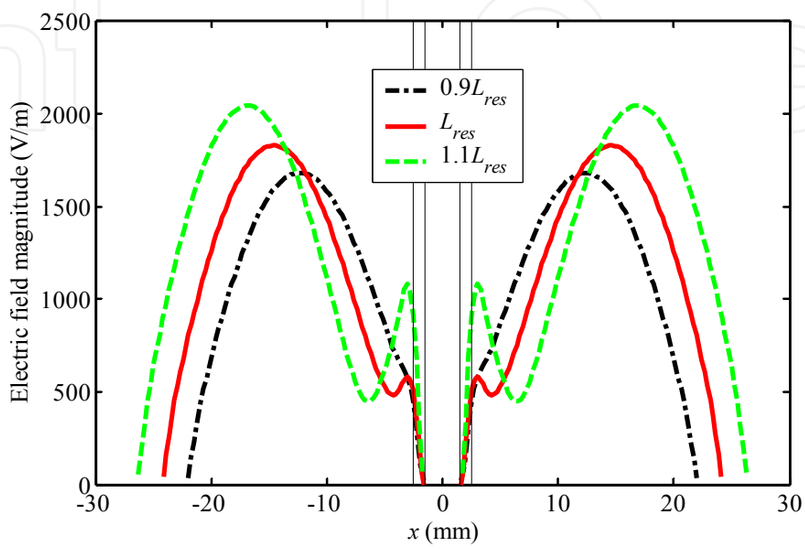

Fig. 2. Magnitude of electric field of isolated slots with half-lengths in vicinity of second-resonance half-length L_{res}. L_{res} = 21.75 mm, W = 1 mm, l_s = 19.4 mm = 0.48 λ_{CPW}, h = 1.575 mm, ε_r = 2.33, w = 3 mm, s = 1 mm. Vertical lines correspond to position of CPW.

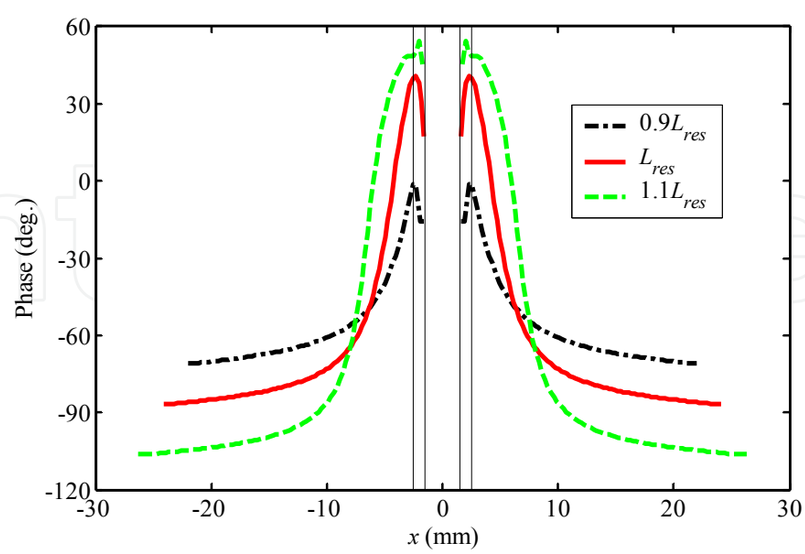

Fig. 3. Phase of electric field of isolated slots with half-lengths in vicinity of second-resonance half-length L_{res}. L_{res} = 21.75 mm, W = 1 mm, l_s = 19.4 mm = 0.48 λ_{CPW}, h = 1.575 mm, ε_r = 2.33, w = 3 mm, s = 1 mm. Vertical lines correspond to position of CPW.

Contrary to the nearly constant phases of CPW-fed slots with half-lengths in the vicinity of the first-resonant half-length (Jacobs, 2007), the phases of these second-resonant slots exhibit a sharp rise close to the CPW feed line, while changing little in the outer reaches of the slots. Increases in slot length result in offsets of phases with respect to phases of preceding lengths. Similar graphs were obtained for slots on conductor-backed two-layer substrates (Jacobs, 2007).

3. Mutual coupling between CPW-fed slots

The focus of this section is the calculation of mutual coupling between slot pairs in linear arrays of slots fed in series by CPW. The geometry of such an array, designed for a broadside main lobe, is shown in Fig. 4. While a variety of types of CPW-fed slot arrays have been reported, for instance wideband linear CPW-fed log-periodic dumb-bell slot arrays (Kim et al., 2006), amplifier arrays using CPW-fed folded slot antennas (Tsai et al., 1994), and CPW-fed planar (two-dimensional) slot arrays in multi-chip module-deposition (MCM-D) technology (Soliman et al., 1999), the rigorous calculation of mutual coupling between slot array elements in the context of iterative array design procedures has only rarely been addressed, *e.g.*, Huang et al. (1999). For certain applications, such calculations seem unnecessary: the design of *uniform* CPW-fed arrays on both single-layer substrates (Qui et al., 2002) and conductor-backed two-layer substrates (Jacobs et al., 2003) have been accomplished without explicitly calculating the mutual coupling between individual pairs of slots, as noted earlier. On the other hand, the design of *non-uniform* arrays subject to rigorous sidelobe-level specifications generally requires explicit, accurate accounts of the mutual coupling between all possible slot pairs in the array.

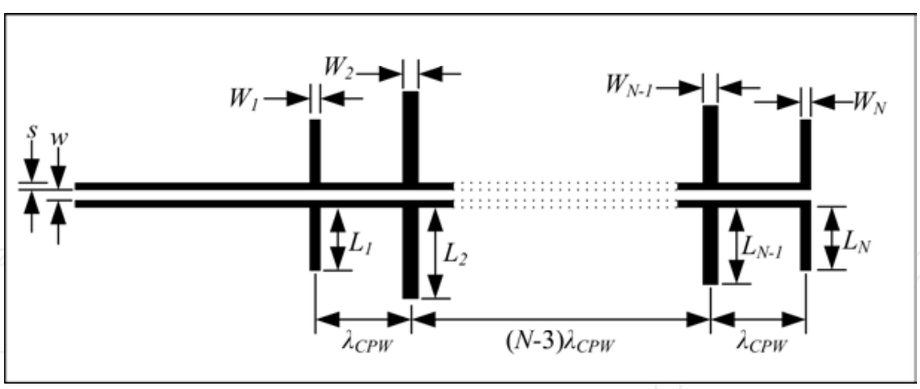

Fig. 4. Top view of N-element CPW-fed linear slot array with equiphase element excitations. L_m ≡ half-length and W_m ≡ width of radiating slot m, where m = 1, 2 .. N; s ≡ slot width and w ≡ center strip width of CPW feed lines; λ_{CPW} ≡ CPW wavelength.

3.1 Mutual coupling between slots on electrically thin single-layer dielectric substrate

For electrically thin substrates a simplified method based on a well-known reciprocity-based expression can be used to find the mutual admittance between two broadside CPW-fed slots (Jacobs & Joubert, 2009a). The method is eminently suitable for easy incorporation into

iterative array design algorithms, and for fast evaluation. The geometry is shown in Fig. 5; slot orientations correspond to their orientation in a linear array such as that of Fig. 4. The slots in Fig. 5 are intended to be accurate models of slots in an array environment – hence their termination in CPW sections implementing short-circuits that extend beyond their radiating portions (this will be more fully described below). The kind of mutual admittance calculation performed here is required when adopting a so-called first-order interaction approach (Amitay et al., 1972) towards finding the mutual admittance between any two slots in an array: the mutual admittance between a specific pair of slots is, for the sake of simplicity, assumed to be identical to the mutual admittance between them when the other slots in the array are removed.

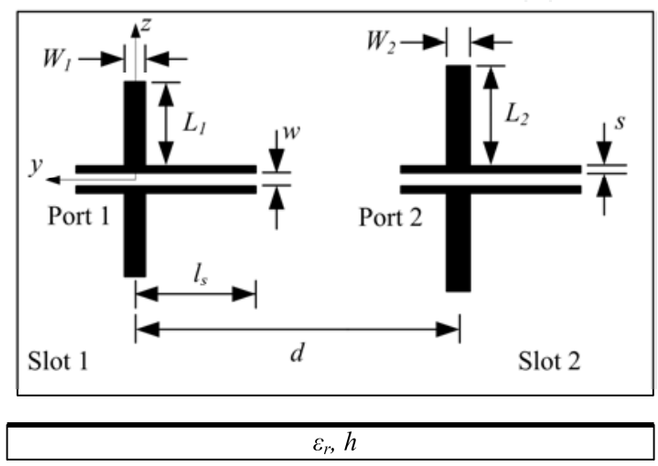

Fig. 5. Top and side views of broadside CPW-fed slots on single-layer dielectric substrate. $L_1 = L_2 \equiv$ half-lengths and $W_1 = W_2 \equiv$ widths of radiating slots; $d \equiv$ distance between radiating slots; $s \equiv$ slot width and $w \equiv$ center strip width of CPW feed lines; $h \equiv$ dielectric layer height; $\varepsilon_r \equiv$ relative dielectric constant; $l_s \equiv$ length of CPW stub implementing short-circuit.

The simplified method assumes that, for mutual admittance calculations between CPW-fed slots on electrically thin single-layer substrates, the inhomogeneous air-dielectric layer-air medium can be sufficiently accurately approximated by a homogenous free space (this is different from the approach taken by Huang et al. (1999)). The mutual admittance between CPW-fed slots *1* and *2* of Fig. 5 can then be found by adapting results originally derived for wire dipoles radiating in free space in (Balanis, 1996) to slots in an infinite ground plane radiating in free space. If it is assumed that CPW feed lines have negligible effect on mutual coupling, only the radiating portions of the CPW-fed slots need to be considered. Hence,

$$Y_{21} = -\frac{1}{V_1 V_2}\left[\int_{-(w/2+s+L_2)}^{-(w/2+s)} H_{z21}(z_2) I_{m2}(z_2)\,dz_2 + \int_{w/2+s}^{w/2+s+L_2} H_{z21}(z_2) I_{m2}(z_2)\,dz_2\right] \tag{1a}$$

where

$$H_{z21}(z_2) = H_r(z_2)\cos\theta - H_\theta(z_2)\sin\theta \tag{1b}$$

with

$$H_r(z_2) = \int_{-(w/2+s+L_1)}^{-(w/2+s)} I_{m1}(z_1)\eta_0 \frac{L_1 \cos\theta}{2\pi r^2}\left[1+\frac{1}{jk_0 r}\right]e^{-jk_0 r}dz_1 + \int_{w/2+s}^{w/2+s+L_1} I_{m1}(z_1)\eta_0 \frac{L_1 \cos\theta}{2\pi r^2}\left[1+\frac{1}{jk_0 r}\right]e^{-jk_0 r}dz_1 \tag{1c}$$

and

$$H_\theta(z_2) = \int_{-(w/2+s+L_1)}^{-(w/2+s)} I_{m1}(z_1) j\eta_0 \frac{k_0 L_1 \sin\theta}{4\pi r}\left[1+\frac{1}{jk_0 r}-\frac{1}{(k_0 r)^2}\right]e^{-jk_0 r}dz_1 + \int_{w/2+s}^{w/2+s+L_1} I_{m1}(z_1) j\eta_0 \frac{k_0 L_1 \sin\theta}{4\pi r}\left[1+\frac{1}{jk_0 r}-\frac{1}{(k_0 r)^2}\right]e^{-jk_0 r}dz_1 \tag{1d}$$

In the above, H_{z21} is the magnetic field of equivalent magnetic current I_{m1} at the position of slot *2* when slot *1* radiates in isolation (I_{m1} represents slot *1* when radiating in isolation), I_{m2} is the equivalent magnetic current representing slot *2* when radiating in isolation, V_1 is the terminal voltage of slot *1* when radiating in isolation, V_2 is the terminal voltage of slot *2* when radiating in isolation, L_1 and L_2 are the half-lengths of slots *1* and *2* respectively, s is the slot width and w the center strip width of the CPW feed line, $r = \sqrt{(z_2 - z_1)^2 + d^2}$, $k_0 = \omega\sqrt{\mu_0 \varepsilon_0}$ is the free-space wavenumber, and $\eta_0 = \sqrt{\mu_0/\varepsilon_0}$ the free-space intrinsic impedance. r and θ are spherical coordinates and the dimensions constituting the integration boundaries are shown in Fig. 5.

The above equations can be implemented as follows to find Y_{21} against slot spacing d for two CPW-fed slots on an electrically thin substrate:

First, each CPW-fed slot of Fig. 5 is simulated in isolation using IE3D (in the case of twin slots, only one slot needs to be simulated). As noted earlier, in order to accurately model a CPW-fed linear array environment, each slot is terminated in a perfect short-circuit realized by a section of transmission line of length l_s, with l_s measured from the center of the radiating portion of the slot. For composite slot (feed line, radiating slot and short-circuit termination) k, where k = 1 or 2, the simulation yields the tangential electric field along the center of the radiating slot (see Figs. 2 & 3), from which its equivalent magnetic current density I_{mk} can be obtained. It is assumed that the radiating slot electric field only has a vector component across the width of the slot (in other words, the small longitudinal component predicted by IE3D is neglected), and that the field is constant across the width of the slot. The latter assumption, which enables calculation of I_{m1} and I_{m2} by simply multiplying the corresponding equivalent magnetic current density by the slot width, can be enforced in IE3D by adopting a discretization that allows for only one cell across the slot width. In addition to the slot tangential field, the isolated-slot moment-method analysis also gives the terminal voltages V_k, where k = 1 or 2. Excitation ports in IE3D are defined at the ends of feed lines (*cf.* Fig. 5). The port voltage computed by IE3D at the end of the feed line

is in fact the terminal voltage, and is found by integrating the transverse electric field in one of the two CPW slots over the slot width. In the mutual admittance calculations described below, terminal voltages (and isolated slot self-admittances) were referred to centers of radiating slots.

Second, Equation (1) was evaluated for each instance of slot separation d. In accordance with the definition of the quantities that constitute equation (1), I_{m1}, I_{m2}, V_1 and V_2 were kept the same for all values of d. Curves of Y_{21} against d obtained with the reciprocity-based method outlined above were compared with curves computed using IE3D. Using a moment-method approach towards this end implies that the entire two-slot structure of Fig. 5 needs to be solved for each instance of d. Ports were defined at the ends of the CPW feed lines, and from the full-wave solution IE3D calculated the two-port Y parameters of the structure with respect to the above ports. Y parameters (including Y_{21}) were afterwards referred to centers of radiating slots.

Y_{21} against d with $0.9\lambda_{CPW} \leq d \leq 2\lambda_{CPW}$ was computed for three pairs of identical broadside (twin) slots on the electrically thin substrate with h = 1.575 mm and ε_r = 2.33 (at 6 GHz, h = $0.048\lambda_d$ = $0.0315\lambda_0$, with λ_d and λ_0 the wavelengths in the dielectric and free space respectively). The slots' widths W was 1 mm, their half-lengths $L_1 = L_2$ were $0.9L_{res}$, L_{res} and $1.1L_{res}$ respectively, with L_{res} = 21. 75 mm, and the length of the short-circuit stub l_s was $0.48\lambda_{CPW}$ = 19.4 mm. The slots were fed by a 87 Ω CPW feed line that had dimensions w = 3 mm and s = 1 mm. The resonant slot had a self-impedance of 17 Ω, and hence can be considered a 'typical' slot from a linear array perspective, given that the input impedance of a broadside CPW-fed linear array is simply the sum of the slots' active impedances, and since slot self-impedance is often considered a first-order approximation to slot active impedance (Elliott, 1981). The self-impedances of the $0.9L_{res}$ and $1.1L_{res}$ slots were 20-j16 Ω and 16+j19 Ω respectively.

The real and imaginary parts of Y_{21} against normalized slot separation d/λ_{CPW} for the twin slots with $L_1 = L_2 = L_{res}$ are shown in Fig. 6; results from both the reciprocity-based method (the curves labeled 'rec.') and IE3D are given. Likewise, Y_{21} against d/λ_{CPW} for twin slots with $L_1 = L_2 = 0.9L_{res}$ and $L_1 = L_2 = 1.1L_{res}$ are shown in Figs. 7 and 8 respectively. The third set of curves (labeled 'improved rec.') in each of Figs. 6–8 correspond to an improved version of the reciprocity-based method that used, instead of the terminal voltages V_k obtained from IE3D, new terminal voltages $V_{k,\,new}$ that were computed as follows. The most accurate results for Y_{21} in a linear array with broadside main lobe are required when the slot spacing $d = \lambda_{CPW}$; this is the minimum spacing between slot elements, and the effect of mutual coupling would be the greatest here. Thus, for each of the twin slot cases represented in Figs. 6–8, the value of Y_{21} was computed at $d = \lambda_{CPW}$ using IE3D; so was the reaction integral in equation (1). The product $V_{1,\,new}\ V_{2,\,new}$ was then obtained from the quotient of IE3D's Y_{21} and the reaction integral value. Since twin slots were involved, $V_{1,\,new}$ and $V_{2,\,new}$ are equal. These voltages were then used in a new evaluation of equation (1) over the range of d.

Figs. 6–8 reveal generally good agreement between Y_{21} computed using the original reciprocity-based method and Y_{21} computed using IE3D, with agreement being best for the $0.9L_{res}$ twin slots and least good for the longest (*i.e.*, $1.1L_{res}$) twin slots. For each of the three cases, the magnitude of the difference between the Y_{21}-against-d curves obtained with the original reciprocity-based method and IE3D were computed, and normalized to the magnitude of the isolated slot self-admittance, $|Y_{self}|$. Averaged over the range of d, the normalized magnitude of the difference was found to be 10.2% for the L_{res} slots, 1.8% for the

$0.9L_{res}$ slots, and 12% for the $1.1L_{res}$ slots. These average errors decreased to 3%, 1.4%, and 2.4% respectively when the improved reciprocity-based method was used. Hence excellent results can be obtained at the cost of further pre-processing required to compute the terminal voltages $V_{1,\ new}$ and $V_{2,\ new}$ in the manner described above. In an actual linear array design, this would need to be done once only, presumably for the same matrix of slot lengths and widths that self-admittance data will be generated for (Huang et al., 1999).

In order to verify the accuracy of IE3D's calculations, Y_{21} against frequency was computed using that simulator for a twin slot configuration with a fixed layout identical to that shown in Fig. 5, except for one of the slots being rotated by 180° in order to enable feeding it from the edge of the substrate via a coaxial launcher. The twin slots were designed to be at their second resonances at 6 GHz, and had $L_1 = L_2 = 20.95$ mm $= L_{res,\ 6\ GHz}$, and $W_1 = W_2 = 1$ mm on an electrically thin substrate with $h = 0.813$ mm, $\varepsilon_r = 3.38 \pm 0.05$ and $\tan\delta = 0.0027$ (*i.e.*, Rogers RO4003C laminate). The feed line characteristic impedance was 83 Ω ($w = 3$ mm and $s = 1$ mm). Fig. 9 shows good agreement between measured and simulated Y_{21} (referenced to the centers of the slots) data.

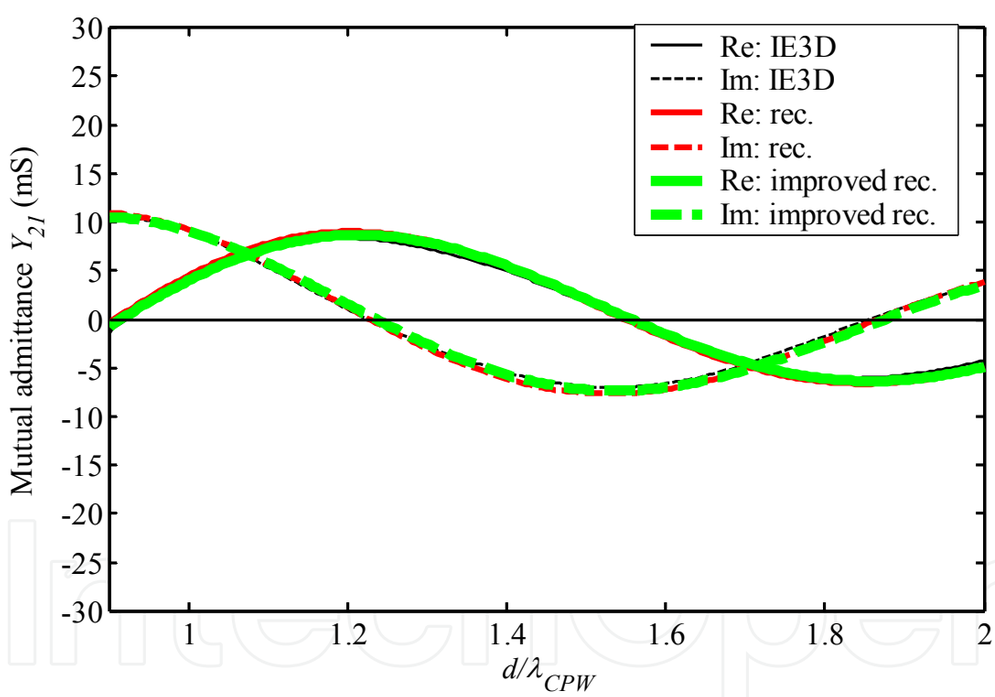

Fig. 6. Mutual admittance Y_{21} against broadside distance d/λ_{CPW} at 6 GHz for CPW-fed twin slots with $L_1 = L_2 = L_{res} = 21.75$ mm. $W_1 = W_2 = 1$ mm, $l_s = 19.4$ mm $= 0.48\ \lambda_{CPW}$, $h = 1.575$ mm, $\varepsilon_r = 2.33$, $w = 3$ mm, $s = 1$ mm.

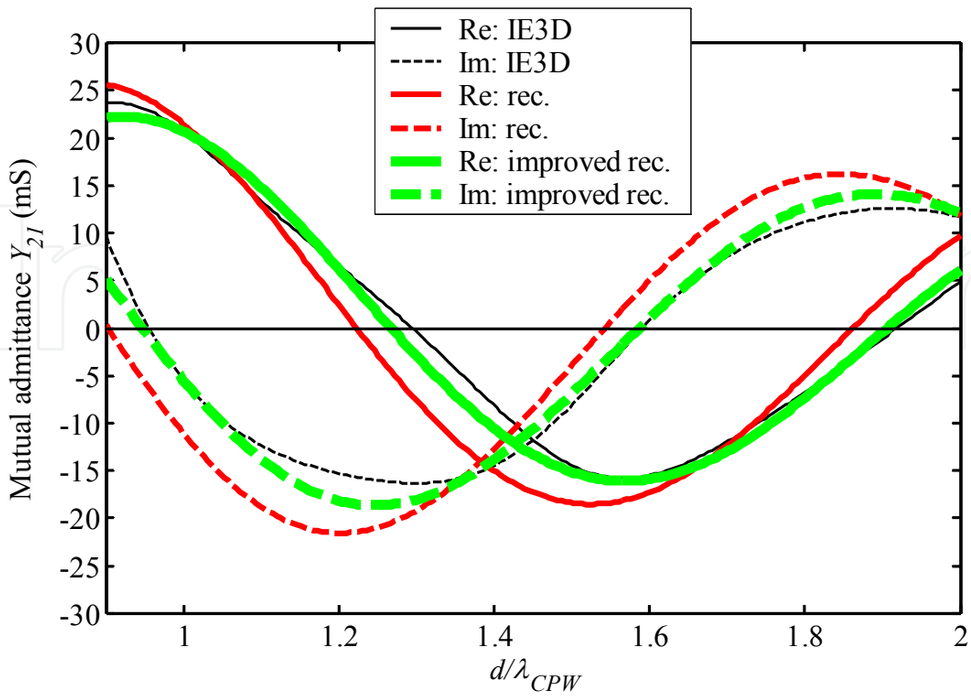

Fig. 7. Mutual admittance Y_{21} against broadside distance d/λ_{CPW} at 6 GHz for CPW-fed twin slots with $L_1 = L_2 = 0.9L_{res}$ = 19.575 mm. $W_1 = W_2$ = 1 mm, l_s = 19.4 mm = 0.48 λ_{CPW}, h = 1.575 mm, ε_r = 2.33, w = 3 mm, s = 1 mm.

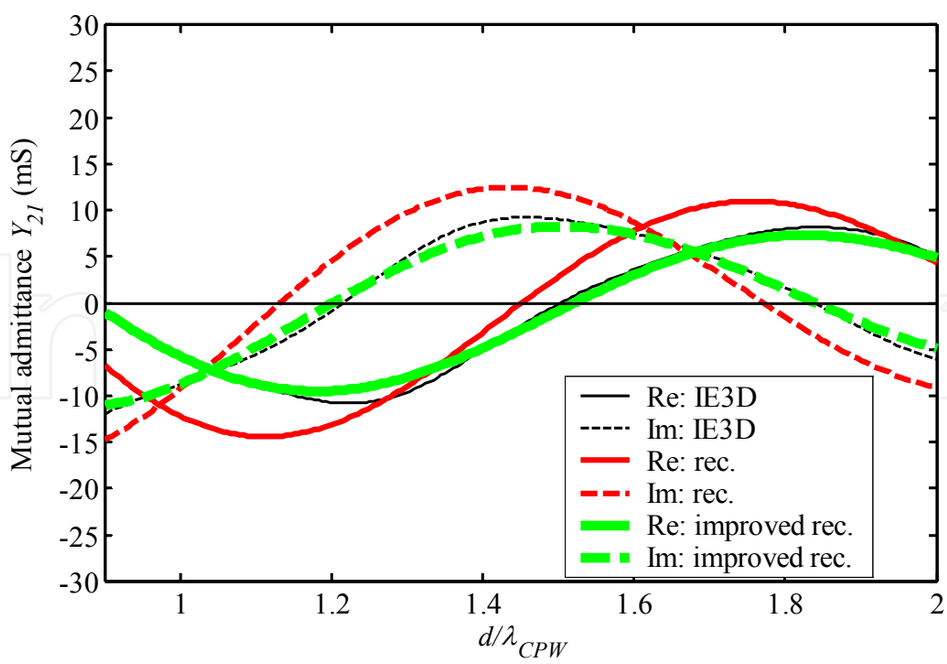

Fig. 8. Mutual admittance Y_{21} against broadside distance d/λ_{CPW} at 6 GHz for CPW-fed twin slots with $L_1 = L_2 = 1.1L_{res}$ = 23.925 mm. $W_1 = W_2$ = 1 mm, l_s = 19.4 mm = 0.48 λ_{CPW}, h = 1.575 mm, ε_r = 2.33, w = 3 mm, s = 1 mm.

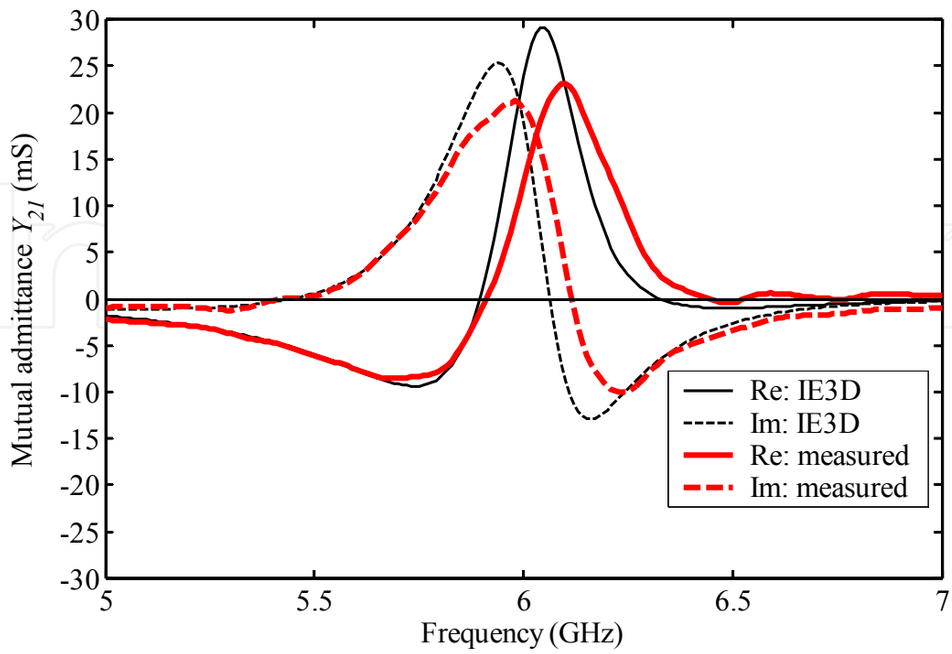

Fig. 9. Computed and measured mutual admittance Y_{21} against frequency for CPW-fed twin slots. $L_1 = L_2 = L_{res,\ 6\ GHz}$ = 20.95 mm, $W_1 = W_2$ = 1 mm, l_s = 18.3 mm = $\lambda_{CPW,\ 6\ GHz}$, $d = \lambda_{CPW,\ 6\ GHz}$ = 38.1 mm, h = 0.813 mm, ε_r = 3.38±0.05, tan δ = 0.0027, w = 3 mm, s = 1 mm.

3.2 Slots on conductor-backed two-layer substrate

Fig. 10 shows twin CPW-fed slots on a two-layer conductor-backed substrate with an air bottom layer (i.e., ε_{r2} = 1). For applications that require unidirectional radiation, this particular structure is of interest as the radiation efficiency attainable with appropriately-spaced twin slots on such a substrate is comparable to that of twin slots on $\lambda_d/4$ single-layer substrates with a reflector positioned $\lambda_o/4$ away from the CPW ground planes side (Qiu et al., 2000) (λ_d is the wavelength in the dielectric; λ_o is the free-space wavelength). This is true even though the substrate of Fig. 10 is of lesser electrical height than the twin slots on a single-layer substrate – potentially an advantage at microwave frequencies.

3.2.1 Effect of conducting back plane

The antenna input impedance of a linear slot array on $\lambda_d/4$ single dielectric substrate is unaffected by a back reflector placed $\lambda_o/4$ on the side of the CPW ground planes (Qiu et al., 2002). This is an indication that the back reflector has minimal influence on mutual coupling between the array slots. However, in this section the presence of a back reflector placed below a two-layer substrate (Fig. 10) is shown to change the mutual coupling between slots. This implies a change in internal coupling (i.e., coupling on the dielectric side) due to the presence of the back plane. Thus, the appropriate parallel-plate two-layer Green's function would be needed in order to account for mutual coupling with sufficient accuracy in an iterative array design procedure (Jacobs et al., 2005).

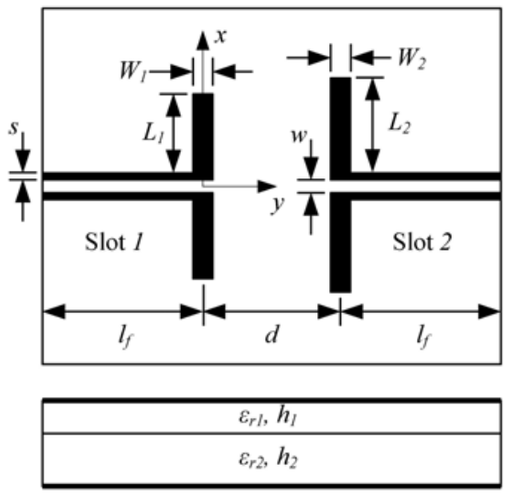

Fig. 10. Top and side views of broadside CPW-fed twin slot antennas on conductor-backed two-layer substrate. $L \equiv$ half-length and $W \equiv$ width of radiating slots; $d \equiv$ distance between radiating slots; $s \equiv$ slot width and $w \equiv$ centre strip width of feed lines; $l_f \equiv$ length of feed lines; h_1 and $h_2 \equiv$ dielectric layer heights; ε_{r1} and $\varepsilon_{r2} \equiv$ relative dielectric constants.

Assuming infinite top and bottom conducting planes and dielectric layers with dielectric constants $\varepsilon_{r1} = 3.38$ and $\varepsilon_{r2} = 1$, with the top substrate layer height $h_1 = 0.813$ mm, simulations were carried out at 10 GHz to demonstrate the effect of back plane height on mutual coupling between the twin slots of Fig. 10 (Jacobs et al., 2005). Three values of bottom layer height, or back plane distance, were considered, namely $h_2 = \infty$, $\lambda_o/4$, and $\lambda_o/6$ (at 10 GHz, $\lambda_o/4 = 7.5$ mm and $\lambda_o/6 = 5$ mm). The case $h_2 = \infty$ is equivalent to the absence of a back plane. A CPW feed line with characteristic impedance of about 50 Ω for the case $h_2 = \infty$ is used (w = 3.7 mm and s = 0.2 mm). For each of the cases $h_2 = \infty$, $\lambda_o/4$, and $\lambda_o/6$, an isolated (radiating) slot with a width W = 0.4 mm was designed to be resonant at 10 GHz by adjusting its half-length L. The resulting resonant slot half-lengths were 10.36 mm, 10.60 mm and 10.67 mm respectively, with corresponding self-impedances of 12.5 Ω, 11.2 Ω, and 13.9 Ω.

Fig. 11 shows the real and imaginary parts g_{21} and b_{21} of the normalized mutual admittance y_{21} as a function of normalized distance d/λ_{CPW} for each of the three cases $h_2 = \infty$, $\lambda_o/4$, and $\lambda_o/6$. y_{21} is the mutual admittance Y_{21} normalized with respect to the relevant isolated resonant slot self-admittance. The reason for normalizing Y_{21} is that, in a linear array context, the relative size of mutual admittance magnitudes with respect to the slots' self-admittance magnitudes is an indicator of the extent of the effect of mutual coupling on the array input impedance.

The normalized curves indicate that, in the absence of a back plane, the maximum values of the magnitudes of the real part (G_{21}) and imaginary part (B_{21}) of the mutual admittance Y_{21} are about 40% and 27% respectively of the resonant slot self-admittance; the maximum of $|g_{21}|$ occurs at $d = \lambda_{CPW}$ and the maximum of $|b_{21}|$ at $d = 1.4\,\lambda_{CPW}$.

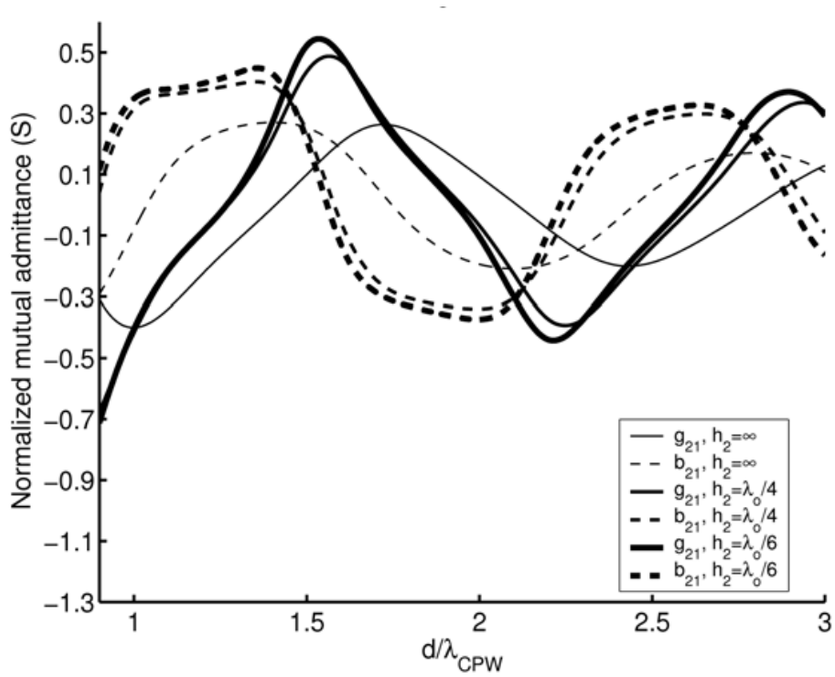

Fig. 11. Real and imaginary parts g_{21} and b_{21} of normalized mutual admittance y_{21} vs. interslot distance d/λ_{CPW} at 10 GHz.

Adding a back plane at $h_2 = \lambda_o/4$ results in significantly higher relative maximum values of about 68% and 40% for $|G_{21}|$ and $|B_{21}|$ respectively; other extrema also show notable increases compared to the $h_2 = \infty$ case. The back plane has the effect of shifting the curves for g_{21} and b_{21} so that their extrema in general are not aligned with those of the curves for $h_2 = \infty$. These effects can be ascribed to internal mutual coupling (the external equivalent problem, concerned with fields in the half-space adjacent to the CPW ground planes, is unchanged by the addition of a back plane), indicating that the input impedance of an array on the single-layer substrate would be significantly affected when a back plane is placed $\lambda_o/4$ away. Decreasing the back plane distance to $h_2 = \lambda_o/6$ results in curves quite similar to, and more or less "in phase" with, the curves for the case $h_2 = \lambda_o/4$ with somewhat higher maximum values for g_{21} and b_{21} (0.71 and 0.45 respectively vs. 0.68 and 0.4), suggesting that the effect of mutual coupling increases as back plane distance decreases. At $d = \lambda_{CPW}$ the magnitude of the real part of the mutual admittance was about 40% of the relevant resonant slot self-admittance for all cases of h_2.

3.2.2 An extended reciprocity-based method for calculating mutual admittance

In this section, a computational strategy based on the well-known expression derived from reciprocity is proposed to calculate the mutual admittance between two CPW-fed slots on conductor-backed two-layer substrates (Jacobs et al, 2009). The formulation iteratively updates the field distribution in both slots to account for the coupling interaction between the slots. The classical reciprocity-based approximation assumes that the field in the slot is the same whether the slot is radiating in isolation or in the presence of a second short-

circuited slot. In cases where mutual coupling is high, such as for resonant-length twin slots, this assumption becomes invalid.

The two CPW-fed slots on a conductor-backed two-layer substrate, as shown in Fig. 10, are center-fed by an infinitesimal voltage source that is placed in the centre of a short section of slotline connecting the two CPW feed line slots at their ends. Employing the standard formulation derived from reciprocity the mutual admittance Y_{12} between them is (Nauwelaers & Van de Capelle, 1988)

$$Y_{12} = -\frac{1}{V_1 V_2} \int_{S_2} \mathbf{H}_{21} \cdot \mathbf{M}_2 dS_2 \tag{2}$$

where $\mathbf{M}_2$ is the equivalent magnetic current density representing slot *2*, V_1 and V_2 are the terminal voltages of slots *1* and *2*, respectively and, assuming that the effects of mutual coupling between CPW feed lines, and between feed lines and radiating slots are negligible, S_2 is the surface area of slot *2*. $\mathbf{H}_{21}$ is the magnetic field at the position of slot *2* due to the equivalent magnetic current density, $\mathbf{M}_1$, representing slot *1*. $\mathbf{H}_{21}$ is calculated as the sum of the internal field (using the Green's function for the conductor-backed two-layer substrate), and the external field (using the free-space Green's function).

The initial estimates for $\mathbf{M}_1$ and $\mathbf{M}_2$ are determined by calculating the electric field distributions in the isolated slots using a moment-method solver e.g. IE3D. The isolated-slot moment-method analysis also yielded the terminal voltages V_1 and V_2.

A schematic representation of CPW-fed twin slots is shown in Fig. 12. In situation *a*, slot *1* is assumed to be excited such that its terminal voltage V_1^a equals V_1 (*i.e.*, the terminal voltage of slot *1* when radiating in isolation), while slot *2* is short-circuited. Hence

$$I_1^a = Y_{11} V_1^a \approx Y_{self} V_1 \tag{3}$$

where I_1^a is the terminal current entering port *1*. The current I_2^a entering port *2* can then be found using (Balanis, 1982) adapted for slots (from its original form for wire dipoles):

$$I_2^a = -\frac{1}{V_2} \int_{S_2} H_{21x} M_{2x} dS_2 \tag{4}$$

where all quantities on the right-hand side are similar in meaning to the corresponding quantities in equation (2). For the first interaction, H_{21x} is the longitudinal component of the magnetic field at the position of slot *2* when slot *1* radiates in isolation with terminal voltage V_1 (and terminal current I_1^a), M_{2x} and V_2 are the equivalent magnetic current density and terminal voltage respectively of slot *2* when radiating in isolation, and S_2 is the surface area of slot *2*. From equations (2) and (4) it follows that

$$I_2^a = V_1 Y_{12} \tag{5}$$

where Y_{12} is the first iteration of the mutual admittance, computed using equation (2) with the field distribution for the slots radiating in isolation.

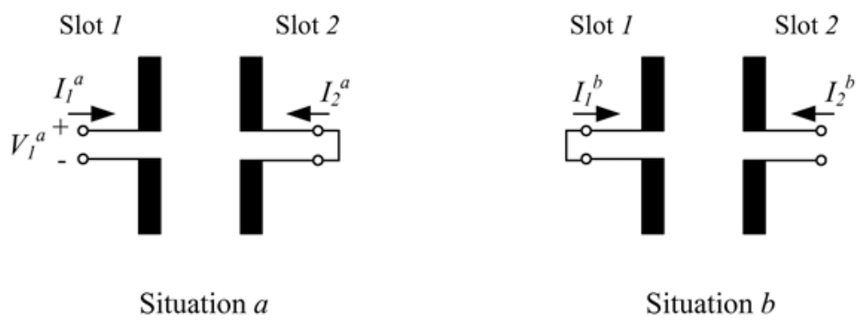

Fig. 12. Schematic representation of CPW-fed twin slots with terminal voltages and currents, and port terminations used in higher-order iterative procedure.

Situation *b* is set up to account for the effect that the current I_2^a induced by slot *1* at the terminals of slot *2* (*cf.* situation *a*) in turn has on slot *1*. Hence slot *2* is assumed to be excited by a terminal current

$$I_2^b = I_2^a \tag{6}$$

while slot *1* is short-circuited. The short-circuit current I_1^b at port *1* can then be found from

$$I_1^b = -\frac{1}{V_1}\int_{S_1} H_{12x}^b M_{1x} dS_1 \tag{7}$$

In the above, H_{12x}^b is the magnetic field at the position of slot *1* when slot *2* radiates in isolation (its terminal current is I_2^b), while M_{1x} and V_1 are the equivalent magnetic current density and terminal voltage respectively of slot *1* when radiating in isolation. Since $H_{12x}^b / I_2^b = -H_{21x} / I_1^a$, it follows from equations (2) and (7) that

$$I_1^b = -\frac{I_2^b}{I_1^a} V_2 Y_{21} \tag{8}$$

with $Y_{21} = Y_{12}$.

The final step in the iterative procedure is to revisit situation *a* and compute updated versions $I_1^{a,update}$ and $V_1^{a,update}$ of the current I_1^a and voltage V_1^a at port *1*:

$$I_1^{a,update} = I_1^a + I_1^b \tag{9}$$

$$V_1^{a,update} \approx \frac{I_1^{a,update}}{Y_{self}} \tag{10}$$

An updated version of the mutual admittance $Y_{12} = Y_{21}$ that includes the effect of the above higher-order interactions between the slots can then be found from

$$Y_{12,update} = Y_{21,update} = \frac{I_2^a}{V_1^{a,update}} \tag{11}$$

while an estimate $Y_{11,est}$ of the two-port self-admittance Y_{11} (at this point only Y_{self} is available) can be computed as follows:

$$Y_{11,est} = \frac{I_1^a}{V_1^{a,update}} \tag{12}$$

The process of updating the two-port admittance parameters can be repeated iteratively until the effect of the next higher-order interaction is negligible.

Fig. 13 shows the Y_{12}-against-d curves for the classical reciprocity approach, the iterative reciprocity-based formulations and a moment-method solver (IE3D) for the case of two identical (twin) resonant slots. Y_{12} against broadside slot separation d was computed at 10 GHz for CPW-fed slots on a conductor-backed two-layer substrate configured for high radiation efficiency. The substrate had h_1 = 0.813 mm = $0.05\lambda_d$, h_2 = 5 mm = $\lambda_0/6$, ε_{r1} = 3.38, and ε_{r2} = 1 (λ_d is the dielectric wavelength in the top layer and λ_0 the free-space wavelength). The substrate allowed for propagation of the TM_0 two-layer parallel-plate mode only. Slot dimensions were W = 0.4 mm and $L = L_{res}$ = 10.87 mm, yielding a resonant self-resistance of 14 Ω; dimensions of the 50 Ω feed line were w = 3.7 mm and s = 0.2 mm.

The extended reciprocity-based curves resemble the shape of the moment-method curves much closer than the classical reciprocity-based curves. The reciprocity-based approach for mutual admittance calculations between CPW-fed slots on conductor-backed two-layer substrates – modified to account for higher-order interactions – is a viable alternative to a moment-method-based approach, offering comparable accuracy and the advantages of simplicity of implementation within iterative array design procedures.

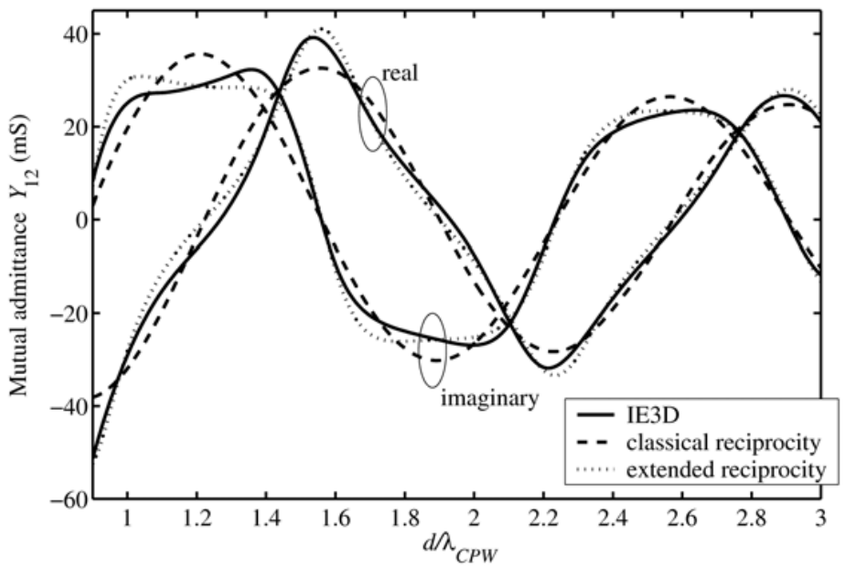

Fig. 13. Mutual admittance Y_{12} against broadside distance d/λ_{CPW} for CPW-fed twin slots with $L_1 = L_2 = L_{res} = 10.87$ mm computed using the classical and extended reciprocity approaches, and IE3D. $W_1 = W_2 = 0.4$ mm; $h_1 = 0.813$ mm; $h_2 = 5$ mm; $\varepsilon_{r1} = 3.38$; $\varepsilon_{r2} = 1$; $l_f = 0.5\lambda_{CPW}$.

4. Linear arrays of CPW-fed slots

4.1 Uniform array on conductor-backed two-layer substrate

This section describes how an approximate iterative design procedure for uniformly-excited CPW-fed linear slot arrays on single-layer substrates (Qiu et al., 2002) can be extended to the case of an 8-element CPW-fed slot array on a conductor-backed higher-lower permittivity two-layer substrate (Jacobs et al., 2003). When designing series-fed broadside linear slot arrays, it is desirable to have slots excited in-phase and with equal magnitude for maximum gain. This implies that slots should be spaced λ_{CPW} rather than $\lambda_g/2$ apart, even though the latter the spacing would seem preferable due to the ensuing phase cancellation of the substrate mode which would result in improved radiation efficiency (λ_{CPW} is the wavelength of the CPW feed line; λ_g is the wavelength of the dominant substrate mode). Previously reported investigations of linear arrays on single-layer substrates, and $\lambda_d/4$ substrates with a back reflector positioned $\lambda_o/4$ away, however indicated that a λ_{CPW} spacing (as opposed to $\lambda_g/2$ spacing) does not affect gain adversely (Qiu et al., 2002).

The top view layout of a generic CPW-fed linear array is shown in Fig. 4; given the present context, all slot half-lengths were assumed to be equal and likewise for slot widths. For simulation purposes, substrate layer heights and dielectric constants were selected (as before) to ensure that a non-leaky CPW feed line would result – this requires a higher-lower permittivity substrate, the higher permittivity layer being adjacent to the slots (Huang & Kuo, 1998). The selected values were $h_1 = 0.813$ mm, $\varepsilon_{r1} = 3.38$, $h_2 = 5$ mm ($\lambda_o/6$ at 10 GHz), and $\varepsilon_{r2} = 1.1$ (see side view in Fig. 10). Using IE3D, a 50 Ω CPW feed line was designed that had $w = 3.7$ mm and $s = 0.2$ mm.

The array (N = 8) was designed for operation at 10 GHz using the following steps in an iterative fashion; the procedure relies on the assumption that slot active impedances are largely determined by the corresponding slot self-impedances (and to a lesser extent by mutual coupling).

1. The self-impedance $Z_{in,slot}$ of a single slot dipole with half-length L and (radiating slot) width W was computed using IE3D (infinite ground planes were assumed throughout). For the first iteration, convenient values of W and L were chosen.
2. An 8-element array was constructed of identical slots spaced λ_{CPW} apart, each with the W and L determined in the previous step. The self-impedance $Z_{in,array}$ of the array was determined using IE3D.
3. The difference Z_{diff} between the array input impedance and the desired input impedance of 50 Ω was found.
4. Using IE3D, new L and W values were found that would yield a new slot self-impedance of $Z_{in,slot} - Z_{diff}/N$.
5. Steps (2) and onwards were repeated until $Z_{in,array}$ was within an acceptable margin from 50 Ω.

The iterative procedure converged to L and W values of 12.04 mm and 1.17 mm respectively. In Fig. 14 measured return loss against frequency is shown for the above design manufactured on a 12″x18″ Rogers RO4003C substrate. The deviation of the measured operating frequency of 9.7 GHz from the design frequency of 10 GHz can be attributed to manufacturing and material considerations that likely included deviations from specified dielectric constants, and inconsistencies in the thickness of the polystyrene bottom layer.

The E-plane co-polarized radiation pattern measured at 9.7 GHz is shown in Fig. 15. Good agreement with the predicted pattern was exhibited, indicating insignificant leakage of the dominant two-layer parallel-plate mode from the sides of the antenna. Sidelobe levels were below -13 dB as expected except for a sidelobe at 85° that had a level of about -10 dB; this could have been caused by an inadvertently-excited higher-order mode on the CPW feed.

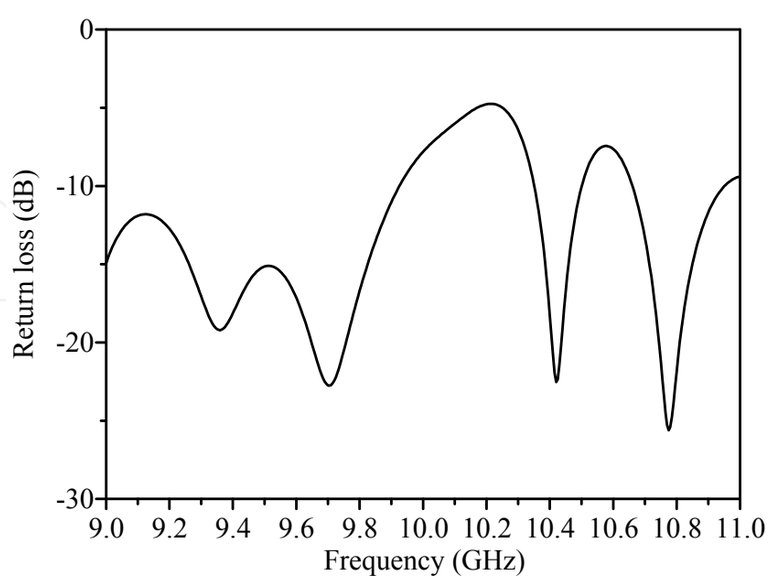

Fig. 14. Measured return loss against frequency for 8-element CPW-fed slot array on conductor-backed two-layer substrate.

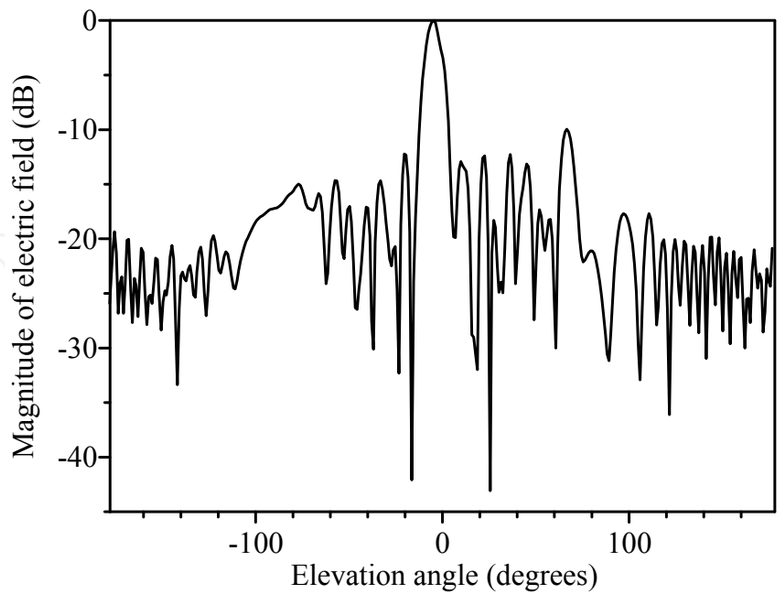

Fig. 15. E-plane co-polarization pattern measured at 9.7 GHz for 8-element CPW-fed slot array on conductor-backed two-layer substrate.

4.2 Non-uniform array on single-layer substrate

This section describes design of a linear non-uniform slot array series-fed by CPW, on an electrically thin substrate for computational simplification, with sidelobe levels substantially reduced beyond that of a uniform array (Jacobs & Joubert, 2009b). The geometry of such a linear array is as shown in Fig. 4. A low-sidelobe level specification typically requires explicit, accurate accounts of the mutual coupling between all possible slot pairs in the array, and hence the ability to enforce a suitably tapered slot excitation. In what follows, the iterative design of a 5-element non-uniform linear CPW-fed array with reduced sidelobe levels on an electrically thin substrate is described. Because of the electrically thin substrate, mutual coupling can be accounted for using the reciprocity-based method involving the assumption of a homogeneous free-space medium, as discussed in section 3.1 (Jacobs & Joubert, 2009a).

4.2.1 Array design procedure

The first step was to synthesize a 5-element Dolph-Tschebychev array of isotropic radiators to have a maximum sidelobe level of -20 dB below the main beam maximum (Balanis, 1996). The spacing between the radiators was $d = 0.78\lambda_0$, with λ_0 the free-space wavelength at the design frequency of 5.6 GHz (this frequency belongs to the upper WLAN band). $0.78\lambda_0$ equals λ_{CPW}, the wavelength of a 70 Ω CPW feed line on a substrate with height h = 1.575 mm and relative permittivity ε_r = 2.33, the substrate of choice for the physical array; the CPW centre strip and slot widths were w = 3 mm and s = 0.5 mm respectively (see Fig. 14). The aim of this particular spacing was to ensure in-phase excitation of the slots. The resulting excitation values were $[V_1\ V_2\ V_3\ V_4\ V_5]$ = [0.52 0.83 1.00 0.83 0.52].

The second step entailed setting up a slot self-admittance database, as well as corresponding field distribution and terminal voltage databases for the calculation of mutual admittances. In particular, self-admittance data was generated using IE3D for a grid of half-lengths and widths of isolated CPW-fed slots: half-length values were between 18.5 and 27.5 mm (at a 0.75 mm interval), and widths were between 0.25 and 3.25 mm (at a 0.25 mm interval). Aperture field and terminal voltage data was collected concurrently with the self-admittance data.

The steps followed in iteratively designing the array are now outlined (see also Huang et al. (1999)) – consider in this regard the generic linear CPW-fed slot array of Fig. 4 that has N slots spaced λ_{CPW} apart with slot half-lengths and widths L_m and W_m (m = 1, 2, ..., N). In network terms, the array can be viewed as an equivalent transmission line circuit with the slots represented by series active impedances separated by λ_{CPW}-long sections of transmission line (Huang et al., 1999; Meide et al., 2002). An active voltage V_m exists across the series active impedance representing slot m, while a current I is common to all slot impedances due to the series nature of the equivalent circuit. The corresponding active admittance of slot m is $Y_m^a = I/V_m$. For an N-element array, the iterative design proceeds as follows:

1. A desired input impedance $Z_{in,des}$ is chosen (50 Ω for the purposes of this letter). The desired slot active admittances $Y_{m,des}^a$ can then be found using the following two equations:

$$Z_{in,des} = \sum_{m=1}^{N} \frac{1}{Y_{m,des}^a} \tag{13}$$

$$Y_{1,des}^a V_1 = \ldots = Y_{N,des}^a V_N \tag{14}$$

2. Starting values for the lengths and widths (L_m, W_m) can then be assumed or calculated. Good starting values can be obtained by initially assuming zero mutual coupling between the slots and then calculating slot dimensions (L_m, W_m) from the self-admittance database that would realize $Y_{mm} = Y_{m,des}^a$.
3. These dimensions (L_m, W_m) are then used to calculate the mutual admittances Y_{mn} between all possible slot pairs m and n according to section 3.1 (Jacobs & Joubert, 2009a). A linear interpolation scheme is used to calculate the updated mutual admittances Y_{mn} during this step for specific (L_m, W_m) dimensions (from the discreet field distribution and terminal voltage database compiled previously).
4. A set of 2N non-linear equations can then be solved to enforce the desired relative slot excitations, the chosen matching criteria, and of course resonance of the N slots in the array. The mutual admittances Y_{mn} are kept constant as calculated in step (3), and a new set of (L_m, W_m) are sought (in effect a new set of self-admittances Y_{mm} are determined) that will satisfy the design equations. The equations are of the form:

$$\frac{Y_m^a}{Y_N^a} = \frac{V_N}{V_m}, \text{ for } m = 1, 2, \ldots, N-1 \tag{15}$$

$$\sum_{m=1}^{N} \frac{1}{Y_m^a} = Z_{in,des} \tag{16}$$

$$\text{Imag}(Y_m^a) = 0, \text{ for } m = 1, \ldots, N \tag{17}$$

Throughout the non-linear equation solving process, a bivariate spline interpolation scheme (McNamara & Joubert, 1994) is used to calculate new self-admittances Y_{mm} for arbitary (L_m, W_m) dimensions, using the previously compiled discreet self-admittance database.

5. Updated mutual admittances for the new slot dimensions can then be calculated, and the true active admittances determined using $Y_m^a = \sum_{n=1}^{N} Y_{mn} \frac{V_n}{V_m}$, from which the actual input impedance of the array can then be found. If Z_{in} is not close enough to the desired value of $Z_{in,des}$, steps 4 and onwards are repeated until convergence is obtained.

4.2.2 Results and discussion

Application of the above procedure yielded the following dimensions for the $N = 5$ array: $L_1 = L_5 = 23.9$ mm, $W_1 = W_5 = 0.3$ mm, $L_2 = L_4 = 23.1$ mm, $W_2 = W_4 = 1.15$ mm, and $L_3 = 23.1$ mm, $W_3 = 2.2$ mm. For the purpose of simulating the full array in IE3D, a short-circuit stub termination of length $l_s = 21$ mm $\approx \lambda_{CPW}/2$ was added (see Figure 4), as well as a front-end CPW feed section of length $\lambda_{CPW}/2$. The simulated array was etched on a Rogers RT/duroid 5870 laminate ($h = 1.575$ mm, $\varepsilon_r = 2.33 \pm 0.02$, $\tan\delta = 0.0009$) of dimensions 230 mm × 135 mm (see Figure 16), and its reflection coefficient, radiation patterns and gain were measured.

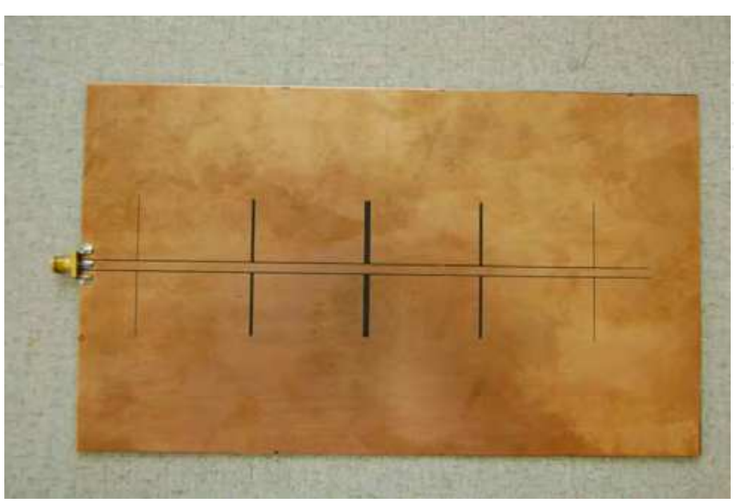

Fig. 16. The manufactured 5-element CPW-fed array.

Fig. 17 shows the simulated and measured array reflection coefficient against frequency. The simulated and measured resonant frequencies were 5.61 GHz and 5.59 GHz respectively, which are both very close to the design frequency of 5.6 GHz. The simulated fractional bandwidth was 1.5% (VSWR < 2), while the corresponding measured bandwidth was 2.1%, confirming the inherently narrow-band nature of the feeding scheme. Discrepancies between simulation and measurement can likely be attributed to manufacturing errors.

Fig. 18 displays the simulated and measured normalized E-plane radiation patterns (the array lies in the xy plane). The simulated co-polarization pattern has a maximum sidelobe level of about -17 dB, which is higher than the designed-for Dolph-Tschebychev sidelobe level of -20 dB. This can be attributed to the accuracy of mutual admittance calculations. The measured co-polarized pattern on the whole agrees well with the simulated pattern (the discontinuity in the simulated pattern at Theta = ±90˚ is due to IE3D setting the electric field component perpendicular to the infinite ground plane, *i.e.*, the co-polarized component, to zero at far-field observation points coinciding with the ground plane; this apparently is an artifact of the simulator). The somewhat higher maximum sidelobe levels of about -16 dB in the measurement can possibly be attributed to the finite substrate (simulations were carried out for a laterally infinite substrate). Fig. 18 also gives the measured cross-polarization which is significantly below co-polarization levels (simulated cross-polarization was too small to show on this graph).

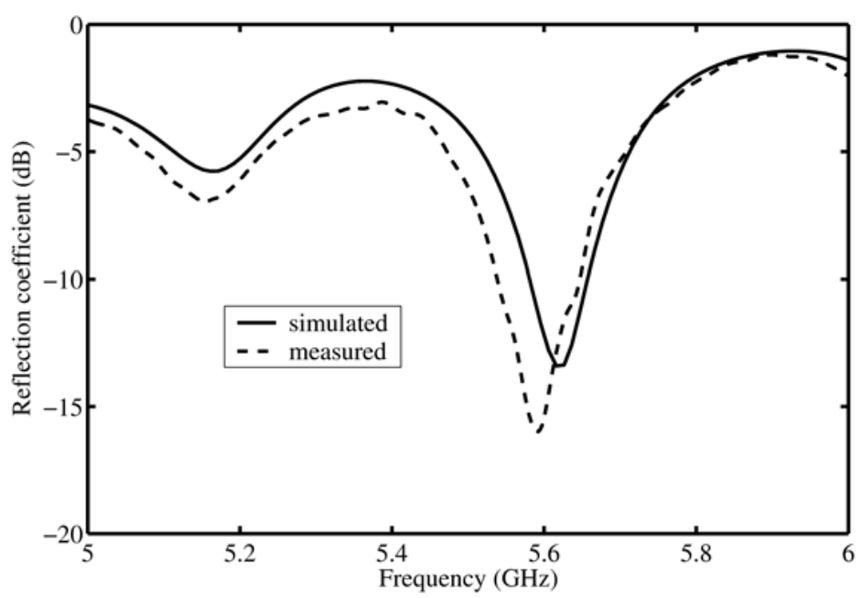

Fig. 17. Simulated and measured reflection coefficient vs. frequency.

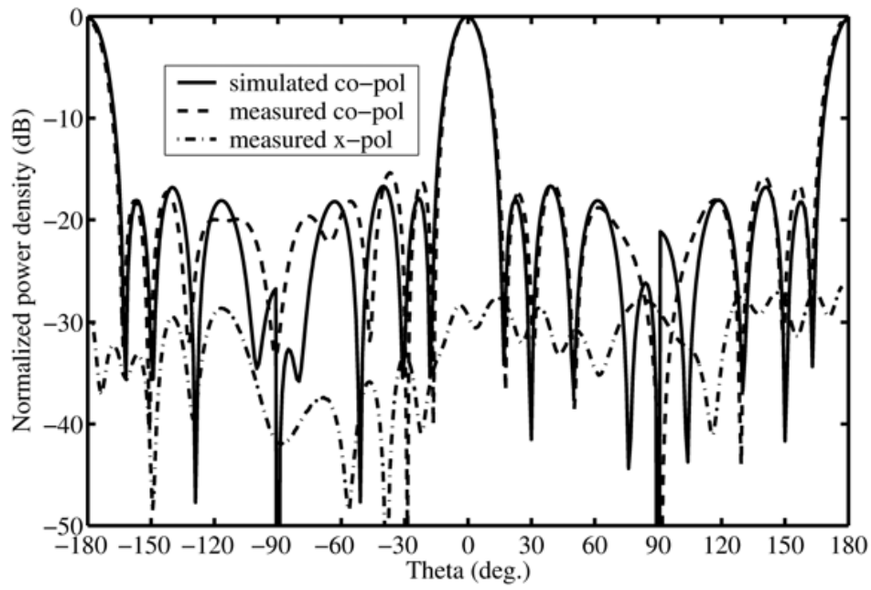

Fig. 18. Simulated and measured E-plane radiation patterns.

The maximum boresight gain of the array is at 5.62 GHz, *i.e.*, 14 dBi (predicted) and 13.5 dBi (measured). The corresponding radiation efficiency was calculated using IE3D to be 97%, indicating negligible power loss to substrate modes due to the electrically thin substrate.

5. Final remarks

The design of non-uniform linear CPW-fed slot arrays with sidelobe levels significantly reduced below that of uniform arrays was presented; efficient methods for accomplishing important parts of the design, such as the calculation of mutual coupling subject to representative substrate configurations, were summarized. Results of a practical implementation on an electrically thin single-layer dielectric substrate was shown; measured sidelobe levels of -16 dB below could be achieved.

6. References

Amitay, N.; Galindo, V. & Wu, C. P. (1972). *Theory and analysis of phased array antennas*, Wiley-Interscience, ISBN 10: 0471025534, New York.

Balanis, C. A. (1996). *Antenna theory: analysis and design*, 2nd ed., ISBN-10: 0471592684, Wiley, New York.

Chen, S.-Y.; Lan, I.-C. & Hsu, P. (2007). In-Line Series-Feed Collinear Slot Array Fed by a Coplanar Waveguide, *IEEE Transactions on Antennas and Propagation,* Vol. 55, No. 6, pp. 1739-1744, ISSN: 1350-2417.

Chen, W.-S. & Wong, K.-L. (2000). A dual-frequency coplanar waveguide-fed slot antenna, *Microwave and Optical Technology Letters*, Vol. 25, No. 3, pp. 226–228, ISSN: 0895-2477.

Elliott, R. S. (1981). *Antenna theory and design*, Prentice-Hall, ISBN: 0130383562, Englewood Cliffs, New Jersey.

Focardi, P.; Neto, A. & McGrath, W. R. (2002). Coplanar-waveguide-based tetraherts hot-electron-bolometer mixers – improved embedding circuit description, *IEEE Transactions on Microwave Theory and Techniques,* Vol. 50, pp. 2374–2383, ISSN: 0018-9480.

Huang, J.-F. & Kuo, C.-W. (1998). More investigations of leakage and nonleakage conductor-backed coplanar waveguide. *IEEE Transactions on Electromagnetic Compatibility*, Vol. 40, No. 3, pp. 257-261, ISSN: 0018-9375.

Huang, T.-F.; Lu, S.-W. & Hsu, P. (1999). Analysis and design of coplanar waveguide-fed slot antenna array, *IEEE Transactions Antennas and Propagation*, Vol. 47, No. 10, pp. 1560-1565, ISSN: 0018-926X.

Jacobs, J. P. (2007). Self and mutual admittance of CPW-fed slots on conductor-backed two-layer substrates, *Microwave and Optical Technology Letters*, Vol. 49, No. 11, pp. 2798–2802, ISSN: 0895-2477.

Jacobs J. P. & Joubert, J. (2009a). Fast and efficient calculation of mutual admittance between CPW-fed slots on electrically thin substrates, *International Journal of RF and Microwave Computer-Aided Engineering*, Vol. 19, No. 2, pp. 277-284, ISSN: 1096-4290.

Jacobs J. P. & Joubert, J. (2009b). Design of a linear nonuniform CPW-fed slot array with reduced sidelobe levels, *Microwave and Optical Technology Letters*, Vol. 51, No. 9, pp. 2175-2178, ISSN: 0895-2477.

Jacobs, J. P.; Joubert, J. & Odendaal, J. W. (2003). Conductor-backed CPW-fed broadside linear slot antenna array on two-layer dielectric substrate, *Proceedings of International ITG-Conference on Antennas*, pp. 61–63, Berlin, Sep. 2003, Germany.

Jacobs, J. P.; Joubert, J. & Odendaal, J. W. (2005). Effect of back plane distance on mutual coupling between CPW-fed slots on conductor-backed two-layer substrates. *Microwave and Optical Technology Letters,* Vol. 47, No. 5, pp. 407-409, ISSN: 0895-2477.

Jacobs, J. P.; Joubert, J. & Odendaal, J. W. (2009). Extended reciprocity-based computation of mutual admittance between CPW-fed slots on conductor-backed two-layer substrates. *Microwave and Optical Technology Letters*, Vol. 51, No. 1, pp. 91-94, ISSN: 0895-2477.

Kim, S. H.; Choi, J. H.; Baik, J.W. & Kim, Y. S. (2006). CPW-fed log-periodic dumb-bell slot antenna array, *Electronics Letters*, Vol. 42, No. 8, pp. 436–438, ISSN: 0013-5194.

McNamara D. A. & Joubert, J. (1994). On the use of bivariate spline interpolation of slot data in the design of slotted waveguide arrays, *ACES Journal*, Vol. 9, No. 1, pp. 6-9, ISSN: 1054-4887.

Miao, M.; Ooi, B. L. & Kooi, P. S. (2000). Broadband CPW-fed wide slot antenna, *Microwave and Optical Technology Letters,* Vol. 25, No. 3, pp. 206–211, ISSN: 0895-2477.

Nauwelaers, B. K. J. C. & Van de Capelle, A. R. (1988). Integrals for the mutual coupling between dipoles or between slots: with or without complex conjugate. *IEEE Transactions on Antennas and Propagation,* Vol. 36, No., 10, pp. 1375-1381, ISSN: 0018-926X.

Neto, A.; De Maagt, P. & Maci, S. (2003). Optimized basis functions for slot antennas excited by coplanar waveguides, *IEEE Transactions on Antennas and Propagation*, Vol. 51, No. 7, pp. 1638–1646, ISNN: 1350-2417.

Qiu, M.; Simcoe, M. & Eleftheriades, G. V. (2000). Radiation efficiency of printed slot antennas backed by a ground reflector, *Proceedings of 2000 IEEE Antennas and Propagation Society International Symposium,* pp. 1612-1615, ISBN: 0-7803-6372-8, Salt Lake City, July 2000, USA.

Qiu, M.; Simcoe, M. & Eleftheriades, G. V. (2002). High-gain meanderless slot arrays on electrically thick substrates at millimeter-wave frequencies, *IEEE Transactions Microwave Theory and Techniques*, Vol. 50, No. 2, pp. 517–528, ISSN: 0018-9480.

Soliman, E. A.; Brebels, S.; Beyne, E. & Vandenbosch, G. A. E. (1999). 2x2 and 4x4 arrays of annular slot antennas in MCM-D technology fed by coplanar CPW networks, *IEE Proceedings Microwaves, Antennas and Propagation*, Vol. 146, No. 5, pp. 335–338, ISSN: 1350-2417.

Tsai, H. S.; Rodwell, M. J. W. & York, R. A. (1994). Planar amplifier array with improved bandwidth using folded-slots, *IEEE Microwave and Guided Wave Letters*, Vol. 4, No. 4 pp. 112–114, ISSN: 1051-8207.

Zeland Software (2001). IE3D User's Manual, Release 8.

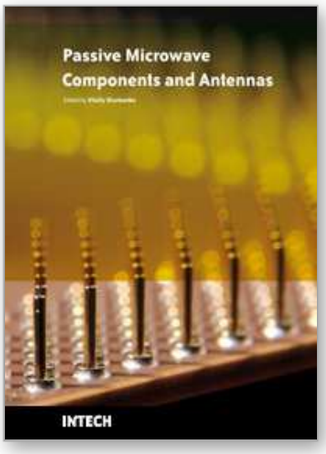

Passive Microwave Components and Antennas

Edited by Vitaliy Zhurbenko

ISBN 978-953-307-083-4
Hard cover, 556 pages
Publisher InTech
Published online 01, April, 2010
Published in print edition April, 2010

Modelling and computations in electromagnetics is a quite fast-growing research area. The recent interest in this field is caused by the increased demand for designing complex microwave components, modeling electromagnetic materials, and rapid increase in computational power for calculation of complex electromagnetic problems. The first part of this book is devoted to the advances in the analysis techniques such as method of moments, finite-difference time- domain method, boundary perturbation theory, Fourier analysis, mode-matching method, and analysis based on circuit theory. These techniques are considered with regard to several challenging technological applications such as those related to electrically large devices, scattering in layered structures, photonic crystals, and artificial materials. The second part of the book deals with waveguides, transmission lines and transitions. This includes microstrip lines (MSL), slot waveguides, substrate integrated waveguides (SIW), vertical transmission lines in multilayer media as well as MSL to SIW and MSL to slot line transitions.

How to reference

In order to correctly reference this scholarly work, feel free to copy and paste the following:

JP Jacobs, J Joubert and JW Odendaal (2010). Design of Non-Uniformly Excited Linear Slot Arrays Fed by Coplanar Waveguide, Passive Microwave Components and Antennas, Vitaliy Zhurbenko (Ed.), ISBN: 978-953-307-083-4, InTech, Available from: http://www.intechopen.com/books/passive-microwave-components-and-antennas/design-of-non-uniformly-excited-linear-slot-arrays-fed-by-coplanar-waveguide

INTECH
open science | open minds

InTech Europe
University Campus STeP Ri
Slavka Krautzeka 83/A
51000 Rijeka, Croatia
Phone: +385 (51) 770 447
Fax: +385 (51) 686 166
www.intechopen.com

InTech China
Unit 405, Office Block, Hotel Equatorial Shanghai
No.65, Yan An Road (West), Shanghai, 200040, China
中国上海市延安西路65号上海国际贵都大饭店办公楼405单元
Phone: +86-21-62489820
Fax: +86-21-62489821

© 2010 The Author(s). Licensee IntechOpen. This chapter is distributed under the terms of the Creative Commons Attribution-NonCommercial-ShareAlike-3.0 License, which permits use, distribution and reproduction for non-commercial purposes, provided the original is properly cited and derivative works building on this content are distributed under the same license.